Thermochemistry of monocharged anion substitutions in ionic solids

Leslie Glasser[1] ⬤

Abstract

Modification of materials to achieve specific changes in their physical and chemical properties often involves the substitution of ions. While this process is commonly discussed in structural terms, our recent publication focussed on exploring the thermochemical consequences, including enthalpy, entropy, heat capacity, and formula unit volume, associated with substituting monocharged cations for sodium ions as a reference set. In the current study, we extend our analysis to investigate the consequences of substituting monocharged anions, specifically the halides F^-, Br^-, and I^-, as well as H^-, OH^-, and NO_3^-, for chloride anions. This exploration is conducted through least-squares regression analysis of data obtained from 431 chloride ion-exchanged materials. In the case of cation substitutions, the regression trendlines for different substitutions appear to be roughly parallel to each other but vertically displaced. For anion substitutions, however, the trendlines for enthalpy and formula unit volume exhibit a fan-like spread from their data origin. We delve into the reasons behind this observed difference. A detailed analysis of a few outliers is undertaken to identify potential reasons for the discrepancies. These findings contribute to a better understanding of the implications and variations in ion substitutions, shedding light on the intricacies of material modification processes.

Keywords Anions · Enthalpy · Entropy · Heat capacity · Formula unit volumes · Diadochy

Introduction

There are many natural materials in which ions are commonly substituted for one another with important resultant effects on their chemical, physical, electronic, and optical properties [1, 2] but only minor changes in the crystal structures involved. A technical term used for such one-to-one ion substitution is "diadochy" [3]. Such substitutions are often explained in structural terms by the Goldschmidt rules [4–6] and by the Pauling rules [7] which are based on the relative sizes of the ions together with the necessity for charge balance [8]. For example, Mg^{2+} and Fe^{2+} substitution may occur within the spinel mineral system, in spinel itself ($MgAl_2O_4$) and in magnetite ($FeAl_2O_4$), as well as in many other mineral systems.

Corresponding structural considerations apply in biomineralisation [9, 10]. Hydroxyapatite is an important mineral component of vertebrate bones and teeth with possible substitution among hydroxide, OH^-, and carbonate, CO_3^{2-}, anions together with charge balance requirements. Similarly, in the shells of molluscs such as oysters and clams, carbonate ions may be substituted by the charge-equivalent sulphate anions, SO_4^{2-}. Such substitutions will affect the biological and physiochemical behaviour of the material.

While these structural effects have long been considered by synthetic chemists and physicists in attempting to impart desired properties to a given material, less consideration has been given to the thermochemical implications of ion substitution. Following initial publications by Liebman et al. [11–13], we have recently published a comprehensive discussion of the thermochemical consequences of the substitution of monocharged *cations* [3]. The current contribution complements this by consideration of the thermochemical consequences for the comparison of enthalpy, H; entropy, S; heat capacity, C_p; and formula unit volume, V_m of substitution of the monocharged *anions* F^-, Cl^-, Br^-, I^-, H^-, OH^-, and NO_3^- using chloride ion as an arbitrary but convenient reference ion. This extends the initial comparison by Meot-Ner et al. [14] of anion substitution, in the case of CN^- for Cl^-.

✉ Leslie Glasser
 leslieglasser@yahoo.co.uk; l.glasser@curtin.edu.au

1 Curtin Institute for Computation, Discipline of Chemistry, Curtin University, GPO Box U1987, Perth, WA 6845, Australia

Thermochemistry of anion substitution

For the current analysis, we have selected the chloride ion–containing materials, including some hydrates, having accompanying thermochemical data from the "HSC Chemistry" database [15]. Four hundred and thirty-one such chlorides were identified. The ion-substituted chemical formulae were then generated in Excel by substituting the Cl symbols with the appropriate X symbol (F^-, Cl^-, Br^-, I^-, H^-, OH^-, and NO_3^-), and their thermochemical data was then obtained from the same database. The derived material formulae did not always have corresponding thermochemical data available— for example, only 8 hydroxides were usable for enthalpy and only 7 for formula unit volume comparisons—which reduces the range of ion substitutions which can be examined. In the following diagrams, a thermochemical parameter (H, S, C_p, or V_m) of the X-containing material is plotted against the same parameter of the chloride-containing material. The chloride-containing materials are arbitrarily used as references because it is a wide-ranging set. Note that the data for the chloride-containing materials themselves are not plotted but would lie exactly on the diagonal for each chart.

Figure 1 plots the formation enthalpies of each of the X-containing materials against those of the chloride-containing materials. It is noticeable that the data lie on lines which fan slightly out from the origin towards their more negative (and thus more stable) limits. In order to emphasise the behaviour, trendlines for some of the data sets are drawn. The parameters (slope, intercept, and square of the regression coefficient) are listed in Table 1 for each of the linear trendline equations.

The data for entropies are plotted in Fig. 2, those for heat capacities in Fig. 3, and for formula unit volumes in Fig. 4. The fan shape spreading from the origin which is observed also appears prominently in Fig. 4 for the formula unit values.

Discussion and conclusions

The pattern of behaviour between cation- and anion-substituted materials is significantly different in that the trendlines for the former [3] were all vertically displaced, whereas the anion-substituted trendlines fan out from their origins for the enthalpies and formula unit volumes but are parallel for entropies and heat capacities. Vertical displacement arises from additive behaviour on exchanging cations. On the other hand, the trendline slope alterations for anion exchange seem to imply that there is a change in the interaction between the anions replacing the chloride ion which affects the slope — attractive when the smaller fluorides replace chlorides, so increasing the slope for enthalpies, and repulsive when the larger halides replace chlorides, so increasing the trendline slopes for formula unit volumes (cf. Table 1).

Fig. 1 The standard formation enthalpies per anion, $\Delta_f H$/kJ mol^{-1}, at 298 K for materials containing the unit-charged anions X^- (F^-, Br^-, Cl^-, H^-, OH^-, and NO_3^-) with an extensive range of cations, including some hydrates, plotted against the corresponding formation enthalpies of the chloride-containing materials. The symbols for the halogen-related materials are filled, while those for the remaining materials (H^-, OH^-, and NO_3^-) are unfilled
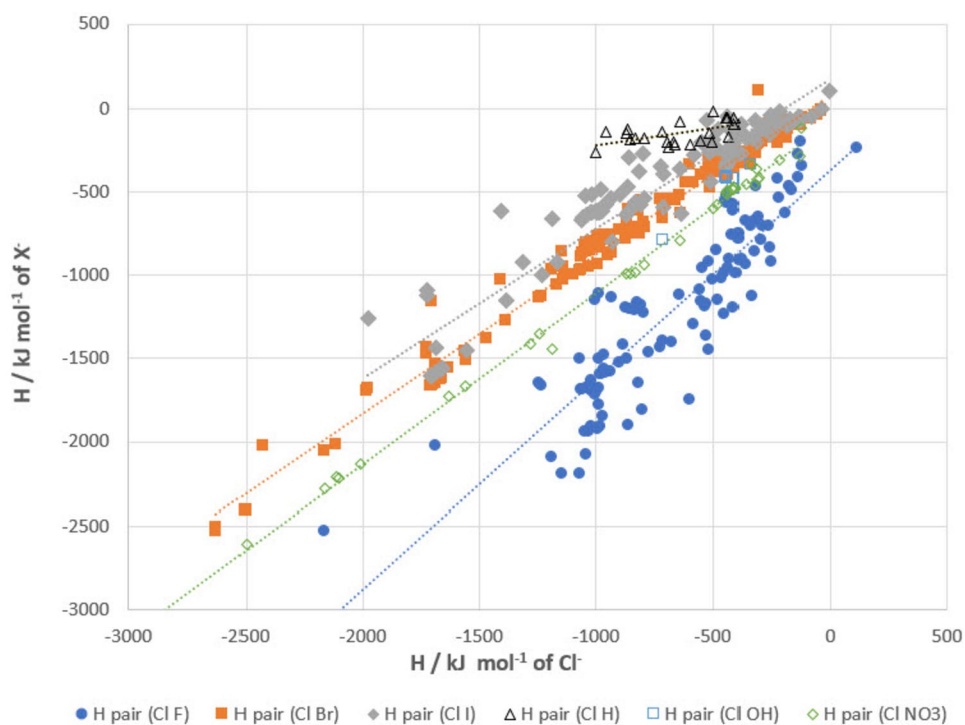
Table 1 Slopes, intercepts, and squared correlation coefficients for linear least-squares regressions for enthalpy, H; entropy, S; heat capacity, C_p; and formula unit volume, V_m, all at 298 K, between monocharged anion-containing ionic solids against the corresponding solids with anions containing chlorides. The missing thermochemistry parameters for anions with chlorides replaced indicate a lack of systematic relations. These linear regressions are plotted in detail in the Supporting Information file

Anion vs. Cl⁻	No. of pairs compared	H/kJ mol⁻¹		
		Slope	Intercept	R^2
F⁻	111	1.256	−368.93	0.79
Br⁻	147	0.956	83.46	0.98
I⁻	108	0.900	174.94	0.90
H⁻	25	–	–	–
OH⁻	8	1.207	83.94	0.93
NO₃⁻	35	1.025	−81.10	0.99

Anion vs. Cl⁻	No. of pairs compared	S/J K⁻¹ mol⁻¹		
		Slope	Intercept	R^2
F⁻	111	0.772	−0.83	0.82
Br⁻	145	0.952	13.22	0.91
I⁻	108	1.029	38.15	0.84
H⁻	25	–	–	–
OH⁻	8	1.108	−18.22	0.81
NO₃⁻	35	1.205	49.16	0.94

Anion vs. Cl⁻	No. of pairs compared	C_p/J K⁻¹ mol⁻¹		
		Slope	Intercept	R^2
F⁻	96	0.886	4.18	0.94
Br⁻	100	0.992	3.38	0.96
I⁻	77	0.988	4.61	0.95
H⁻	24	–	–	–
OH⁻	7	–	–	–
NO₃⁻	18	1.262	42.77	0.920

Anion vs. Cl⁻	No. of pairs compared	V_m/nm³		
		Slope	Intercept	R^2
F⁻	66	0.488	0.01	0.67
Br⁻	70	0.995	0.18	0.82
I⁻	56	1.452	0.00	0.94
H⁻	75	–	–	–
OH⁻	7	1.008	−0.01	0.78
NO₃⁻	17	1.165	0.02	0.92

Hydrides

The ion-substituted hydrides do not relate well to one another in a linear least-squares regression probably because they are not strongly ionic and rather exhibit considerable covalency [16, 17].

Outliers relative to chlorides

In order to illustrate a possible (valuable if minor) use of these charts, in Figs. 3 and 4, we have named a few prominent outliers from their data set trendlines. Such anomalous values may be worthy of further investigation as indicating a special feature of the data or possible data errors. The published set of additive single-atom thermochemical values [18] has here proven to be a reliable check on outlier values.

Heat capacities of AmI₃, AmBr₃, and PtBr₃

It has earlier been noted [19] that ambient heat capacities and entropies of ionic solids are approximately equal and

Fig. 2 The standard formation entropies per anion at 298 K, S/J K^{-1} mol^{-1}, for materials containing the unit-charged anions X$^-$ (F$^-$, Br$^-$, Cl$^-$, H$^-$, OH$^-$, and NO$_3^-$) with an extensive range of cations, including some hydrates, plotted against the corresponding chloride-containing materials. The symbols for the halogen-related materials are filled, while those for the remaining materials (H$^-$, OH$^-$, and NO$_3^-$) are unfilled. The distinct vertical lower limit to the data represents the smallest chloride values in the data set
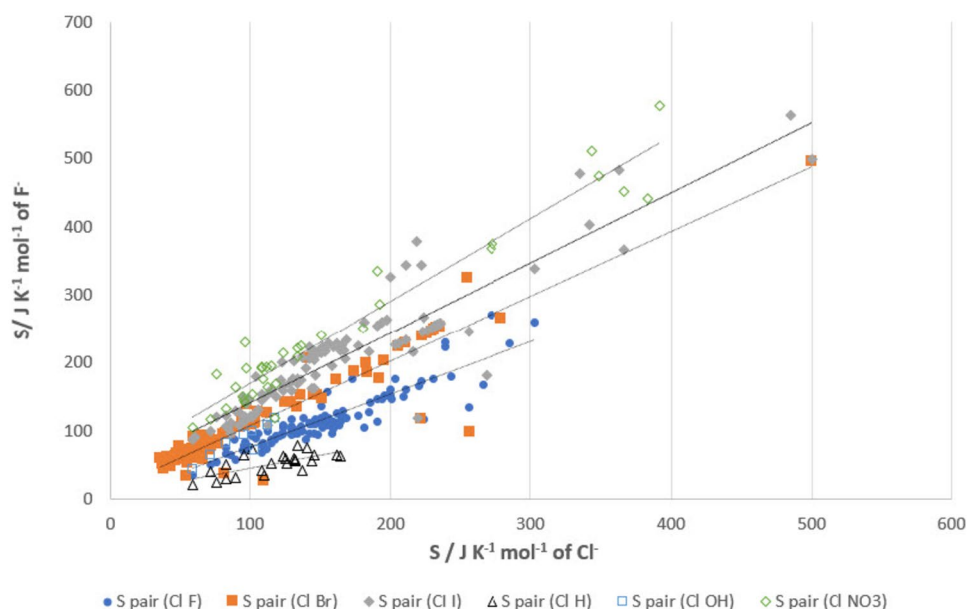
the slopes of linear regression trendlines in Figs. 3 and 4 are roughly equal in accordance with this observation. Table 2 lists the graphed data values of outliers that have been

identified in Fig. 3. If the highlighted anomalous C$_p$ values are replaced by their corresponding C$_p$(atom) values[18], the anomalies are successfully removed from the graph.

Fig. 3 The standard heat capacities per anion at 298 K, C$_p$/J K^{-1} mol^{-1}, for materials containing the unit-charged anions X$^-$ (F$^-$, Br$^-$, Cl$^-$, H$^-$, OH$^-$, and NO$_3^-$) with an extensive range of cations, including some hydrates, plotted against the corresponding chloride-containing materials. The symbols for the halogen-related materials are filled, while those for the remaining materials (H$^-$, OH$^-$, and NO$_3^-$) are unfilled. The data points of some principal outliers are marked: they represent the heat capacities per anion of the noted material and of its chloride-referenced counterpart. The distinct vertical lower limit to the data represents the smallest chloride values in the data set
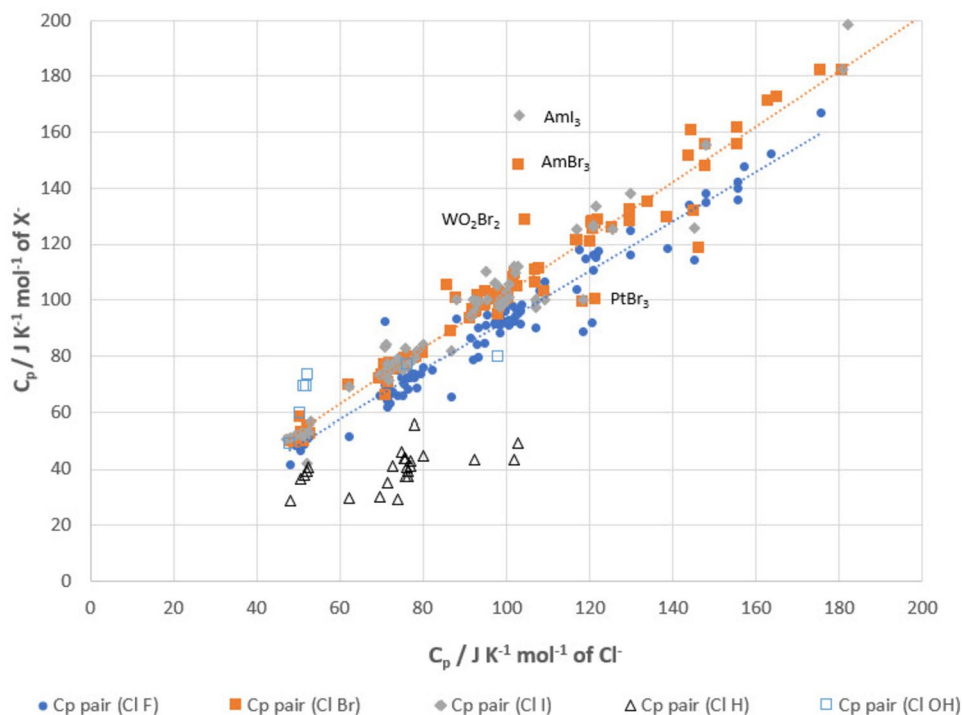
Fig. 4 The formula unit volumes per anion under ambient conditions, V_m/nm^3, for materials containing the unit-charged anions X^- (F^-, Br^-, Cl^-, H^-, OH^-, and NO_3^-) with an extensive range of cations, including some hydrates, plotted against the corresponding chloride-containing materials. The symbols for the halogen-related materials are filled, while those for the remaining materials (H^-, OH^-, and NO_3^-) are unfilled. The distinct vertical lower limit to the data represents the smallest chloride values in the data set
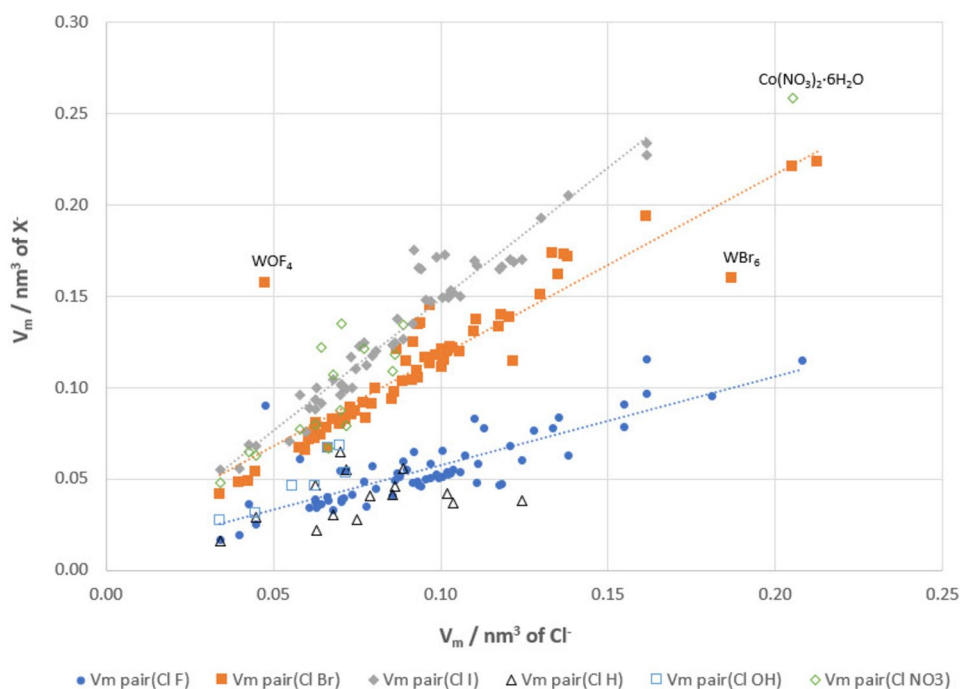
Formula unit volumes of WBr_6, $WOBr_4$, and $Co(NO_3) \cdot 6H_2O$

Formula unit volumes are most readily determined from their densities using the formula $V_m/nm^3 = MW(X)/(602.2 \times \rho/g\ cm^3)$ as in the column "V_m(HSC)" of Table 3. For the outliers labelled in

Fig. 4 and listed in Table 3, the V_m(atom) volumes [18] are satisfactory replacements. A literature data search for $Co(NO_3) \cdot 6H_2O$ failed to find an improved formula unit volume. In fact, this data point is not an outlier but is simply a far-extended value.

Table 2 The table lists some anomalous heat capacity values (/J K^{-1} mol^{-1}) for data points which are labelled in Fig. 3. The column headed "C_p(HSC)" lists graphed values[15], "C_p(atom)" lists calculated additive atom contributions [18], and "Dulong-Petit asymptote" lists the classical limit of $(n \times 25)$ J K^{-1} mol^{-1} where "n" is the number of atoms in the chemical formula, while the final column lists the ratio of column 2 to column 3. Entries in italics represent significant deviations from the expected regular values

Outlier	C_p(HSC)	C_p(atom)	Dulong-Petit asymptote	C_p(HSC)/C_p(atom)
AmI_3	*166.00*	115.27	100	*1.44*
$AmCl_3$	103.00	110.44	100	*0.93*
$AmBr_3$	*148.00*	114.67	100	*1.29*
AmF_3	-	100.78	100	-
WBr_6	182.15	183.06	200	1.00
WCl_6	175.42	174.60	200	1.00
WO_2Br_2	128.40	112.92	125	*1.14*
WO_2Cl_2	104.41	110.10	125	0.95
$PtBr_3$	100.37	98.50	100	1.02
$PtCl_3$	*121.34*	94.27	100	*1.29*

Table 3 The Table lists some anomalous formula unit volumes (/nm^3) for data points which are highlighted in Fig. 4. The column headed "V_m(HSC)" lists graphed values [15], and "V_m(atom)" lists calculated additive atom contributions [18]. The final column lists the ratio of column 2 to column 3. The entries for the hydrates in column 3 under "V_m(atom)" are the volume sums of the parent and of its waters of hydration at a mean value of 22.23 nm^3 for each water molecule [18] [20]. Entries in italics represent significant deviations from the expected regular values

	V_m(HSC)	V_m(atom)	V_m(HSC)/V_m(atom)
WBr_6	*0.1596*[a]	0.2297	*0.69*
WCl_6	0.1871	0.1898	0.99
$WOBr_4$	*0.1568*[b]	0.1683	0.93
$WOCl_4$	*0.0476*	0.1416	*0.34*
$Co(NO_3)_2$	*0.1220*	0.1066	*1.14*
$Co(NO_3)_2 \cdot 6H_2O$	0.2584	0.2400[c]	1.08
$CoCl_2$	0.0642	0.0681	0.94
$CoCl_2 \cdot 6H_2O$	0.2054	0.2015[c]	1.02

[a]There is an updated formula unit volume for WBr_6 of 0.2069 nm^3[21] with V_m(HSC)/V_m(atom) = 0.90

[b]There is an updated formula unit volume for $WOBr_4$ of 0.1312 nm^3[22] with V_m(HSC)/V_m(atom) = 0.78

[c]Vm(atom) recorded for the hydrate is the sum of the values for the parent anhydrate plus six water molecules

Declarations

Ethics approval Not applicable.

Competing interests The authors declare no competing interests.

References

1. Byeon Y-W, Gong M-J, Cai Z, Sun Y, Szymanski NJ, Bai J, Seo D-H, Kim H (2023) Effects of cation and anion substitution in $KVPO_4F$ for K-ion batteries. Energy Storage Materials 57:81–91. https://doi.org/10.1016/j.ensm.2023.02.007

2. Li J, Liu Z, Zhang Q, Cheng Y, Zhao B, Dai S, Wu H-H, Zhang K, Ding D, Wu Y, Liu M, Wang M-S (2019) Anion and cation substitution in transition-metal oxides nanosheets for high-performance hybrid supercapacitors. Nano Energy 57:22–33. https://doi.org/10.1016/j.nanoen.2018.12.011

3. Glasser L, Liebman JF (2024) Thermochemistry of monocharged cation substitutions in ionic solids. Struct Chem. https://doi.org/10.1007/s11224-023-02272-3

4. Wikipedia - Goldschmidt classification. https://en.wikipedia.org/wiki/Goldschmidt_classification. Accessed August, 2023

5. University of Buffalo - Goldschmidt rules. https://www.nsm.buffalo.edu/courses/gly206/TraceChem.pdf. Accessed January, 2024

6. George J, Waroquiers D, Di Stefano D, Petretto G, Rignanese G-M, Hautier G (2020) The limited predictive power of the Pauling rules. Angew Chem Int Ed 59(19):7569–7575. https://doi.org/10.1002/anie.202000829

7. Wikipedia - Pauling's rules. https://en.wikipedia.org/wiki/Pauling%27s_rules. Accessed January, 2024

8. Colson R Mineralogy: substitution rules. https://earthsci4teachers.com/ESE2/Mineralogy_Substitution_Rules/index.html. Accessed January, 2024

9. Bigi A, Boanini E, Gazzano M (2016) Chapter 7 - Ion substitution in biological and synthetic apatites. In: Aparicio C, Ginebra M-P (eds) Biomineralization and biomaterials. Woodhead Publishing, Boston, pp 235–266. https://doi.org/10.1016/B978-1-78242-338-6.00008-9

10. Estroff LA (2008) Introduction: biomineralization. Chem Rev 108(11):4329–4331. https://doi.org/10.1021/cr8004789

11. Liebman JF, Scheiner S (1999) Does thermochemical mimicry extend to Gibbs energies? The differences of K+ and NH4+, and of Na+ and H3O+. Struct Chem 10(5):391–392. https://doi.org/10.1023/A:1022051829674

12. Jenkins HDB, Liebman JF, Ponikvar M, Scheiner S (2009) The heat capacities and standard entropies of corresponding potassium and ammonium ion species: is there a constant difference? Struct Chem 20(1):31–35. https://doi.org/10.1007/s11224-008-9402-z

13. Vegas Á, Liebman JF, Jenkins HDB (2012) Unique thermodynamic relationships for $\Delta_f H^o$ and $\Delta_f G^o$ for crystalline inorganic salts. I. Predicting the possible existence and synthesis of Na_2SO_2 and Na_2SeO_2. Acta crystallographica Section B, Structural science 68(5):511–527. https://doi.org/10.1107/S0108768112030686

14. Meot-Ner M, Cybulski SM, Scheiner S, Liebman JF (1988) Is cyanide significantly anisotropic? Comparison of cyanide vs chloride: clustering with hydrogen cyanide and condensed-phase thermochemistry. J Phys Chem 92(10):2738–2745. https://doi.org/10.1021/j100321a009

15. Metso: Outotec (2022) HSC chemistry. Metso: Outotec Research Oy. https://www.mogroup.com/portfolio/hsc-chemistry/. Accessed March, 2022

16. Glasser L, von Szentpaly L (2006) Born-Haber-Fajans cycle generalized: linear energy relation between molecules, crystals, and metals. J Am Chem Soc 128(37):12314–12321. https://doi.org/10.1021/ja063812p

17. von Szentpaly L (2008) Atom-based thermochemistry: crystal atomization and sublimation enthalpies in linear relationships to molecular atomization enthalpy. J Am Chem Soc 130(18):5962–5973. https://doi.org/10.1021/ja710852w

18. Glasser L (2022) Additive single atom values for thermodynamics I: volumes, entropies, heat capacities of ionic solids. J Chem Thermodynam 166:106685. https://doi.org/10.1016/j.jct.2021.106685

19. Glasser L (2013) Ambient heat capacities and entropies of ionic solids: a unique view using the Debye equation. Inorg Chem 52(11):6590–6594. https://doi.org/10.1021/ic400617u

20. Glasser L (2019) The effective volumes of waters of crystallization: non-ionic pharmaceutical systems. Acta Crystallogr B 75:784–787. https://doi.org/10.1107/s2052520619010436

21. Willing W, Muller U (1987) Wolframhexabromid. Acta Crystallogr C 43(7):1425–1426. https://doi.org/10.1107/S0108270187091625

22. Hess H, Hartung H (1966) Die Kristallstruktur von Wolframoxidchlorid $WOCl_4$ und Wolframoxidbromid $WOBr_4$. Z Anorg Allg Chem 344(3–4):157–166. https://doi.org/10.1002/zaac.19663440306

Publisher's Note Springer Nature remains neutral with regard to jurisdictional claims in published maps and institutional affiliations.